

## Comparative Analysis of Basic Models and Artificial Neural Network Based Model for Path Loss Prediction

Julia O. Eichie<sup>1, \*</sup>, Onyedi D. Oyedum<sup>1</sup>, Moses O. Ajewole<sup>2</sup>, and Abiodun M. Aibinu<sup>3</sup>

**Abstract**—Propagation path loss models are useful for the prediction of received signal strength at a given distance from the transmitter; estimation of radio coverage areas of Base Transceiver Stations (BTS); frequency assignments; interference analysis; handover optimisation; and power level adjustments. Due to the differences in: environmental structures; local terrain profiles; and weather conditions, path loss prediction model for a given environment using any of the existing basic empirical models such as the Okumura-Hata's model has been shown to differ from the optimal empirical model appropriate for such an environment. In this paper, propagation parameters, such as distance between transmitting and receiving antennas, transmitting power and terrain elevation, using sea level as reference point, were used as inputs to Artificial Neural Network (ANN) for the development of an ANN based path loss model. Data were acquired in a drive test through selected rural and suburban routes in Minna and environs as dataset required for training ANN model. Multilayer perceptron (MLP) network parameters were varied during the performance evaluation process, and the weight and bias values of the best performed MLP network were extracted for the development of the ANN based path loss models for two different routes, namely rural and suburban routes. The performance of the developed ANN based path loss model was compared with some of the existing techniques and modified techniques. Using Root Mean Square Error (RMSE) obtained between the measured and the model outputs as a measure of performance, the newly developed ANN based path loss model performed better than the basic empirical path loss models considered such as: Hata; Egli; COST-231; Ericsson models and modified path loss approach.

### 1. INTRODUCTION

Like other wireless communication systems, GSM depends on the propagation of radio waves within the troposphere, the region of the atmosphere extending from the Earth's surface up to an altitude of about 16 km at the equator or 8 km at the poles [1]. Within the troposphere, the heights of human-made structures and natural terrain elevation vary. The transmission path between a transmitter and a mobile receiver differs in the different areas (urban, suburban and rural areas) and varies from simple line-of-sight path to a path with obstructions such as hills, trees, buildings and other human-made structures. The electric field strength of signals radiated from a transmitter is subject to propagation loss due to reflection, refraction, diffraction, absorption and scattering. Weak received signal and path loss due to the reduction of power density of an electromagnetic wave, as it propagates from the transmitting antenna to the receiving antenna, is of great concern in mobile communication.

Propagation path loss models are useful for prediction of received signal strength at a given distance from the transmitter, estimation of radio coverage areas of Base Transceiver Stations (BTS), frequency assignments, interference analysis, handover optimisation, and power level adjustment [2]. Due to the

---

*Received 6 June 2017, Accepted 29 September 2017, Scheduled 25 October 2017*

\* Corresponding author: Julia Ofure Eichie (juliaeichie@futminna.edu.ng).

<sup>1</sup> Department of Physics, Federal University of Technology, Minna, Nigeria. <sup>2</sup> Department of Physics, Federal University of Technology, Akure, Nigeria. <sup>3</sup> Department of Mechatronics Engineering, Federal University of Technology, Minna, Nigeria.

differences in environmental structures, local terrain profiles and weather conditions, the signal strength and path loss prediction model for a given environment using any of the existing basic path loss models such as the Okumura-Hata's model has been shown to differ from the optimal empirical model [3–6].

Artificial Neural Network (ANN), one of the artificial intelligence techniques, has proven to be effective in the development of models for solving prediction problems. ANN is flexible and has the capability to learn the underlying relationships between the inputs and outputs of a process, without needing the explicit knowledge of how these variables are related [7]. It can therefore be useful in the development of path loss models.

The rest of this paper is organized as follows. Section 2 presents literature review, while Section 3 presents methodology for data acquisition and model development. Results and discussion are presented in Section 4 while conclusion is in Section 5.

## 2. LITERATURE REVIEW

This section has two subsections. Subsection 2.1 presents review of related research works from literature while Subsection 2.2 gives a brief overview of path loss model.

### 2.1. Related Research Works

Usman et al. [8] investigated wireless mobile communication signal strength variation with weather and environmental factor in Bauchi. The research revealed variation of signal strength in different locations but similar values were obtained at different times in the same location. In the study of Sharma and Singh [9], involving measurements on received power strength in urban, suburban and rural regions in Narnaul City, India, it was observed that path loss is less in the rural areas than in sub urban and urban areas. Ayekomilogbon et al. [10] study of signal degradation as a function of leaf density revealed seasonal variability in the effect of tress on radio waves due to variation in the electrical constants (conductivity and permittivity) of the trees. Similarly, Nwawelu et al. [11] revealed that trees and buildings have significant effect on the received power level of wireless mobile network.

Ogbulezie et al. [12, 13] investigated the suitability of two basic propagation models for GSM 900 and 1800 MHz respectively for Port Harcourt and Enugu cities, and for Abuja, Kaduna and Kano cities in Nigeria. Measurements taken in cities were compared against predictions made by the Okumura Hata and COST-231 Hata models, and the classical models were observed to overestimate the path loss in all the cities. Similarly, Chebil et al. [14] investigated path loss models for mobile communications in Malaysia. The results revealed that SUI and COST-231 models overpredicted the path loss while log-normal shadowing and Lee models were in close agreement with the measured path loss. Armoogum et al. [15] carried out a comparative analysis of path loss for 3G networks for urban and rural regions of Mauritius Island, India. The research revealed that path loss is not constant at various locations for a constant distance around the respective Base Transceiver Station (BTS) due to the effect of terrain. Benmus et al. [16] developed an empirical model, using ANN approach, for the prediction of propagation path loss at 900MHz, 1800 MHz and 2100 MHz in Tripoli, Libya. Results revealed that the ANN path loss model had acceptable agreement with the target path loss with MSE values ranging from 3.7 to 6.7.

In an attempt to make some basic path loss models suitable in environment that differs from the environment in which the basic path loss models were developed, Nwalozie et al. [5], Bakinde et al. [6] and Obot et al. [17] added the computed mean squared error (MSE) between measured path loss values and basic model predicted path loss values, to the original basic path loss model equations.

### 2.2. Path Loss Model

Path loss is the reduction in power density of an electromagnetic wave as it propagates through a medium. Path loss for each measurement location is given by [18, 19] as:

$$PL_m \text{ (dB)} = \text{EIRP (dBm)} - P_r \text{ (dBm)} \quad (1)$$

where:

$$\begin{aligned} \text{EIRP}_t &= \text{Effective Isotropic Radiated Power} \\ P_r &= \text{received signal level} \\ \text{EIRP}_t &= P_{\text{BTS}} + G_{\text{BTS}} + G_{\text{MS}} - L_{\text{FC}} - L_{\text{AB}} + L_{\text{CF}} \end{aligned} \quad (2)$$

The computation of path loss for all routes:

$$PL_m \text{ (dB)} = P_{\text{BTS}} + G_{\text{BTS}} + G_{\text{MS}} - L_{\text{FC}} - L_{\text{AB}} + L_{\text{CF}} - P_r \quad (3)$$

where:

$$\begin{aligned} P_r &= \text{received signal level} \\ P_{\text{BTS}} &= \text{transmitter power (dBm)} \\ G_{\text{BTS}} &= \text{transmitting antenna gain (dBi)} \\ G_{\text{MS}} &= \text{receiving antenna gain (dBi)} \\ L_{\text{AB}} &= \text{antenna body loss (dB)} \\ L_{\text{FC}} &= \text{feeder cable loss (dB)} \\ L_{\text{CF}} &= \text{combiner and filter loss (dB)} \end{aligned}$$

A path loss model is a set of mathematical expressions and algorithms used for the characterisation of attenuation (reduction in power density) of an electromagnetic wave as a function of frequency, distance and other conditions in a given environment. The existing path loss models can be categorised into two, namely empirical models and theoretical models.

- (a) Empirical Model: This model is based on observations and measurements. This model takes into account all environmental influences, but its accuracy depends on the similarities between the environment to be analysed and the environment used in the development of the model [20].
- (b) Theoretical Model: This model deals with the fundamental principles of radio wave propagation. It utilises the governing laws of wave propagation to determine the received signal level at a particular location. The model can be applied to different environments without altering the accuracy but it is usually very complex and lack computational efficiency [16].

Since this research is based on observations and measurements, empirical models will be considered, and some of the most frequently used basic empirical path loss model equations [9, 14, 19–21] are as follows:

#### (1) COST-231 Hata model

$$PL_{\text{COST231}} = 46.3 + 33.9 \log_{10}(f) - 13.82 \log_{10}(h_b) - a(h_m) + \{44.9 - 6.55 \log_{10}(h_b)\} \log_{10}(d) + C_M \quad (4)$$

where  $a(h_m) = (1.1 \log_{10}(f) - 0.7)h_m - (1.56 \log_{10}(f) - 0.8)$  and  $C_M = 0$  dB.

#### (2) Hata Model

$$\begin{aligned} PL(\text{suburban})_{\text{Hata}} &= 69.55 + 26.16 \log_{10}(f) - 13.82 \log_{10}(h_b) \\ &\quad + \{44.9 - 6.55 \log_{10}(h_b)\} \log_{10}(d) - 2[\log_{10}(f/28)]^2 - 5.4 \end{aligned} \quad (5)$$

$$\begin{aligned} PL(\text{Rural})_{\text{Hata}} &= 69.55 + 26.16 \log_{10}(f) - 13.82 \log_{10}(h_b) \\ &\quad + \{44.9 - 6.55 \log_{10}(h_b)\} \log_{10}(d) - 4.78(\log_{10}(f))^2 + 18.33(\log_{10}(f)) - K \end{aligned} \quad (6)$$

where  $k = 35.94$ .

#### (3) Egli Model

$$PL_{\text{Egli}} = 20 \log_{10} f + 40 \log_{10} d - 20 \log_{10} h_b + 76.3 - 10 \log_{10} h_m \quad (7)$$

#### (4) Ericsson Model

$$PL_{\text{Ericsson}} = a_0 + a_1 \log_{10}(d) + a_2 \log_{10}(h_b) + a_3 \log_{10}(h_b) \log_{10}(d) - 3.2 (\log_{10}(11.75h_r))^2 g(f) \quad (8)$$

where  $g(f) = 44.49 \log_{10}(f) - 4.78(\log_{10}(f))^2$ ,  $a_0$ ,  $a_1$ ,  $a_2$  and  $a_3$  are constants given in Table 1 [22].

**Table 1.** Values of constants in Ericsson model.

Environment	$a_0$	$a_1$	$a_2$	$a_3$
Suburban	43.20	68.93	12.0	0.1
Rural	45.95	100.60	12.0	0.1

### 3. METHODOLOGY

This section presents method of data acquisition and model development.

#### 3.1. Data Acquisition

The measurement setup for data acquisition consists of a laptop equipped with Ericsson TEMS 9.1.4 drive test software, TEMS handsets and a Global Positioning System (GPS) receiver housed in a vehicle as shown in Figure 1.

Two TEMS mobile phones, one for each of the 2 selected wireless mobile communication networks (A and B) and a GPS, all connected to a laptop equipped with Ericsson TEMS 9.1.4 drive test software,



**Figure 1.** Drive test tools housed in a vehicle.

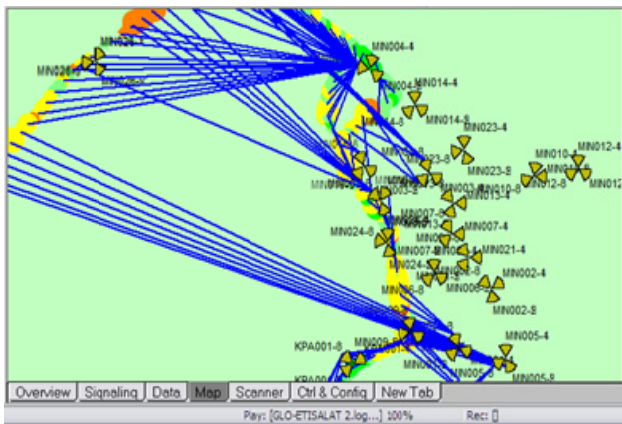


**Figure 2.** Screen shot of measurement points and serving BTS.

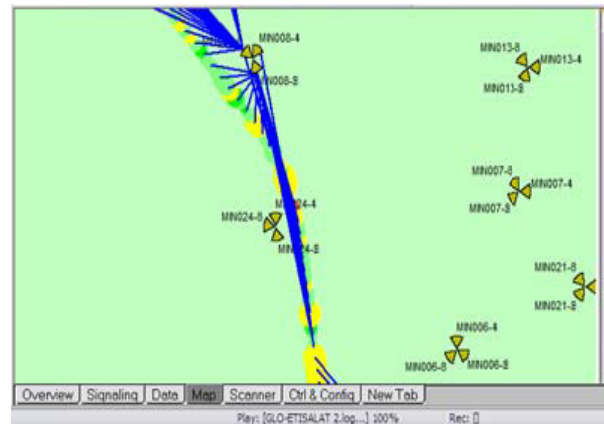


**Figure 3.** Screen shot of a selected BTS (MIN008) serving measurement points.

and housed in a vehicle, were used for drive testing on some selected routes. The mobile phones were positioned at about 1 m distance from the earth surface. The RxLevels of the 2 Networks were measured in the drive test exercise in: the month of April (late dry season); the month of July (early wet season); and the month of October (late wet season) in Niger State. After each drive test exercise, the log files were replayed in TEMS investigation application software. During the replay process, the BTS serving each measurement point were displayed as shown in Figure 2.

Some BTS close to straight or nearly straight rural or suburban routes and serving measurement points without interference from neighbouring cells were selected and used as reference points for measurements. Figure 3 shows one of the selected BTS and the measurement points.

A total of 20 BTS were selected and used in this study. The geographical coordinates of the selected BTS were obtained and used to mark the BTSs locations on Google Earth application software as shown in Figure 4. The elevation above sea level of the marked locations (measurement points) corresponding to each BTS was determined. Each route had 2 reference BTS, 1 for each network. Based on population density, building density, building type and separation between buildings, measurement routes are classified as suburban and rural routes. The routes along which measurements were taken are:

- Rural Routes
  - Along Minna-Zungeru road, Beji
  - Along Minna-Bida road, Gidan Kwanu
- Suburban Routes
  - Along Minna-Bida road, Kpakungu
  - Along Western Bypass road, Dutsen Kura
  - Along Western Bypass road, Gbaiko
  - Along Bahagu Bypass road, Ugwandagi
  - Along Minna-Zungeru road, Tunga
  - Along Minna-Suleja road, Tunga
  - Along Kuta road, Maitumbi
  - Along Minna-Zungeru road, Tudun Fulani



**Figure 4.** Reference BTS points of location (Google Earth, 2016).

The operating frequency,  $f$ , of each of the selected BTS was 1800 MHz, and the receiving antenna height,  $h_m$ , on all routes was approximately 1 m. BTS transmitting power of 40 W was used during the drive test period. Using the TEMS drive test software, the RxLevel at distance intervals of 100 m from each BTS site, up till the cell coverage distance of the respective BTS, was determined for each of the 2 networks.

### 3.2. Model Development

RxLevel variations in relation to elevation above sea level of measurement points were explored on all routes. The distance between each measurement point and its respective reference transmitting antenna, the height of the reference transmitting antenna and the elevation above sea level of measurement points were used as inputs in an MLP network used in the ANN design. The proposed MLP network consists of 3 nodes at the input layer, one hidden layer and 1 node at the output layer. The writing of the script files for the developed path loss models and the performance analysis to determine the weight and bias values, number of neurons and activation function type to be used in the optimal model equations was done using Matlab.

A feedforward network topology and the default Matlab Neural Network Toolbox learning algorithm, Levenberg-Marquardt, were used. The number of neurons in the hidden layer was varied from 31 to 39 in incremental steps of 2. The most frequently used activation functions: logsig, purelin and tansig type of activation functions were used to create the 9 different pairs of activation functions used in the model development. Thus, each of the 5 different numbers of neurons was used with 9 different pairs of activation functions. Each run of the script file generates 45 networks. The script file was run 20 times and 20 runs generated 900 trained networks for performance evaluation. A schematic of the proposed MLP network with variable neurons in the hidden layer is shown in Figure 5, where  $x_i$  (where  $1 \leq i \leq 3$ ) are the set of inputs;  $w_{ij}$  and  $w_{jk}$  are adjustable weight values:  $w_{ij}$  connects the  $i$ th input to the  $j$ th neuron in the hidden layer, and  $w_{jk}$  connects the  $j$ th output in the hidden layer to the  $k$ th node in the output layer;  $y_k$  (where  $k = l$ ) is the output. Each neuron and output node has associated adjustable bias values:  $b_j$  (where  $j =$  number of neurons) is associated with the  $j$ th neuron in network layer 1, and  $b_k$  (where  $k = 1$ ) is associated with the node in the network layer 2. Within each network layer are: the weights,  $w$ , the multiplication and summing operations, the bias,  $b$ , and the activation function,  $\varphi$  [22, 23]. Mathematically, Figure 5 can be represented as Equation (9) [24, 25].

$$y = \varphi_2 \left( \sum_{j=1}^m w_{jk} \varphi_1 \left( \sum_{i=1}^3 w_{ij} x_i + b_j \right) + b_k \right) \tag{9}$$

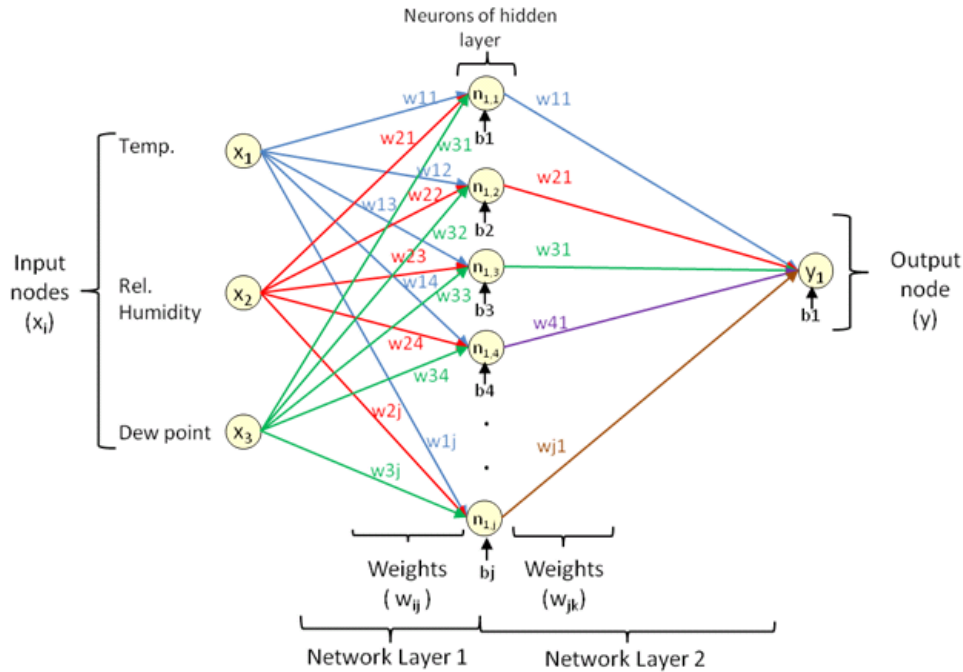


Figure 5. A 2 layered MLP network for path loss model.

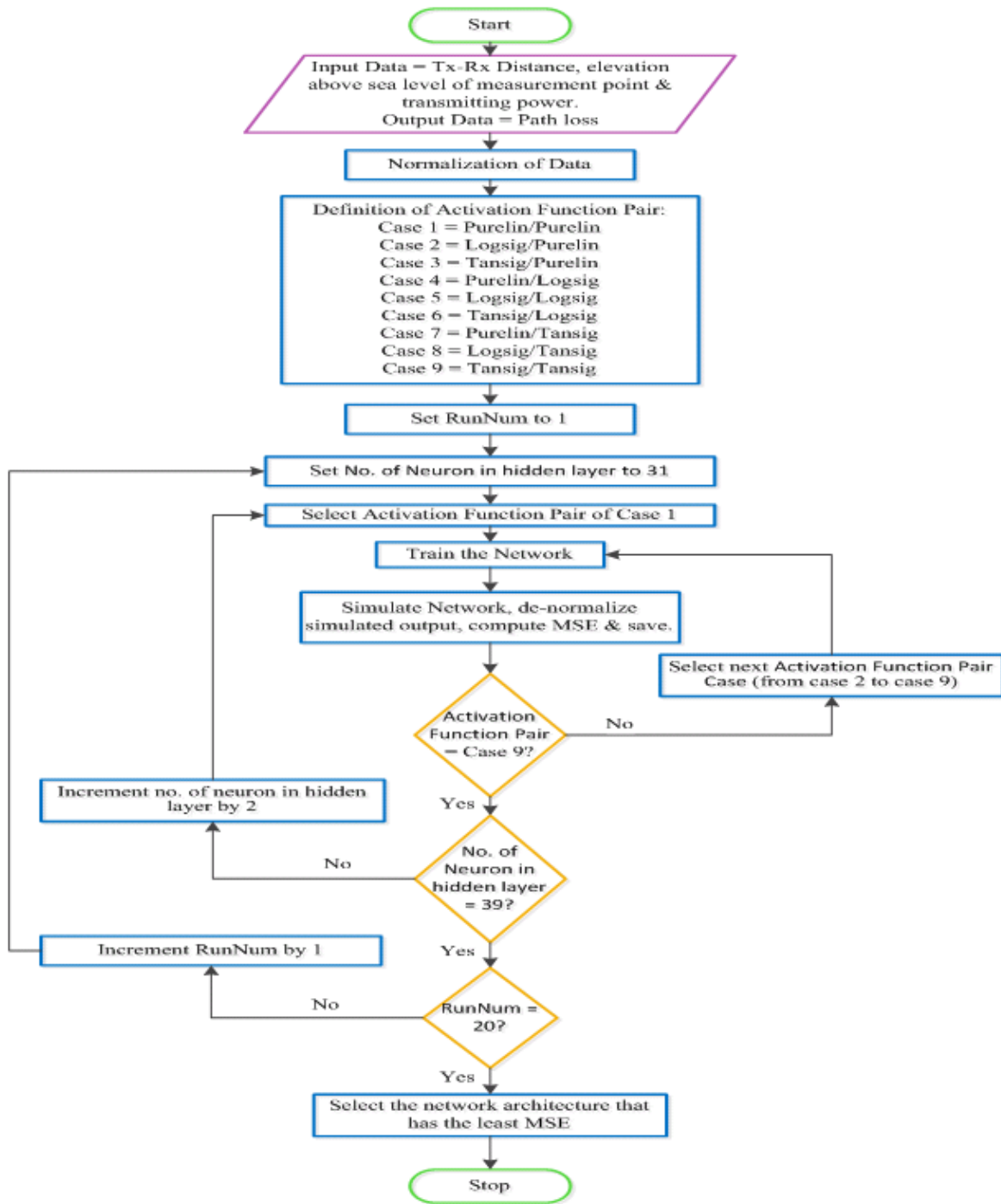


Figure 6. Flow diagram of the ANN script for path loss models.

where  $m$  is the total number of neurons in the hidden layer. The flow diagram of the ANN script file is shown in Figure 6.

Two sets of input/output data were used separately with the ANN script file to develop 2 path loss model equations for rural route and for suburban route. For the rural route path loss model, data from route 1 (76 samples) were used to train the network and for suburban route path loss model data from Network A on routes 3, 5, 7, 9 and 10, and data from Network B on routes 4, 6, 8 and 9 (total of 126 samples) were used while training the network. During the training process, the input and target

output data were applied to the network and the network computed its output. The initial weight and bias values and their subsequent adjustments were done by the Matlab Neural Network Toolbox software. For each set of output in the output data, the error,  $e$ , (the difference between the target output,  $t$ , and the network's output,  $y$ ,) was computed. MSE values were computed and used by the network performance function to optimize the network using Equation (10):

$$\text{MSE} = 1/N \left( \sum_{i=1}^N (t_i - y_i)^2 \right) \quad (10)$$

where  $N$  is the number of sets in the output data,  $t_i$  the target output, and  $y_i$  the network's output.

The weight and bias values were adjusted so as to minimize the MSE and thus increase the network performance. After the adjustments, the network underwent a retraining process, the MSE was recomputed and the weight and bias values were readjusted. The retraining continued until the training data achieved the desired mapping that obtained minimum MSE value. The training and retraining processes were done for each of the 2 sets of input/output data.

#### 4. RESULTS AND DISCUSSION

In this section, performance evaluation results of the developed ANN based path loss model is discussed in Subsection 4.1, while comparison of predicted path loss by ANN based path loss model and some basic empirical path loss models with measured path loss is discussed in Subsection 4.2.

##### 4.1. Evaluation of the Developed Path Loss Models

The network architecture of 9-39-4, with purelin/tansig pair of activation functions, performed best with least MSE value of 24.10 for the rural routes. For the suburban route, network architecture of 1-37-3, with tansig/purelin pair of activation functions performed best with least MSE value of 8.36. Using the weight and bias values, and the architecture of the network with the best performance, the optimal model equations developed for path loss computation in rural and suburban route using transmitting antenna and receiving antenna distance, elevation above sea level of measurement points and transmitting power of reference BTS are:

**Rural route:**

$$y = \frac{2}{1 + \exp(-2((\alpha x - 0.2152) + 0.1205))} - 1 \quad (11)$$

where  $y$  = path loss,  $x$  is a  $(3 \times 1)$  input vector of distance between transmitting and receiving antennas, elevation above sea level of measurement point and transmitting power of reference BTS.  $\alpha$  is a  $(3 \times 1)$  matrix shown in Equation (12).

$$\alpha = [ 0.7068 \quad -0.5988 \quad -0.2808 ] \quad (12)$$

**Suburban route:**

$$y = \alpha \left( \frac{2}{1 + \exp(-2(\beta x + \gamma))} - 1 \right) + 1.1132 \quad (13)$$

where  $y$  = path loss,  $x$  is a  $(3 \times 1)$  input vector of distance between transmitting and receiving antenna, elevation above sea level of measurement point and transmitting power of reference BTS. The constants:  $\alpha$  is a  $(1 \times 37)$  matrix,  $\beta$  is a  $(37 \times 3)$  matrix and  $\gamma$  is a  $(37 \times 1)$  matrix.

Result obtained during the training process of the ANN based path loss model for the rural route is shown in Figure 7, while histogram of the margin of deviation between measured path loss and the predicted path loss is shown in Figure 8.

From Figure 8, margin of deviation within the range of  $-6$  to  $6$  is of high frequency, and it is 86.67% of the total frequency distribution. Margin of deviation within the ranges of  $-7$  to  $-10$  and  $7$  to  $10$  is 13.33% of the total frequency distribution. The margin of deviation and the computed correlation coefficient value of 0.75 show an acceptable accuracy. Figures 9 and 10 show the result of the training process of the ANN based path loss model for the suburban route, and histogram of the margin of deviation between measured and predicted path loss.

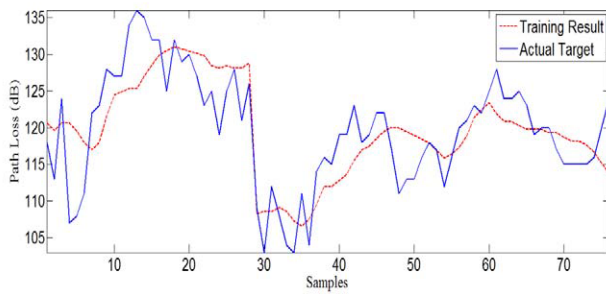


**Figure 7.** Comparison of measured path loss and model predicted path loss (rural route).

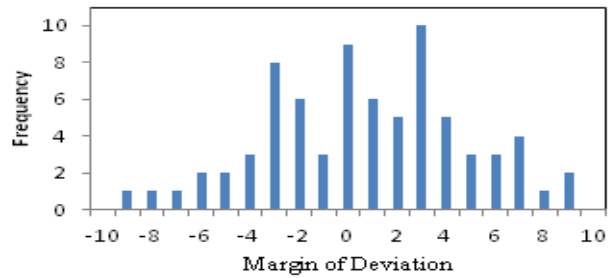


**Figure 8.** Histogram of margin of deviation for ANN path loss model (rural route).

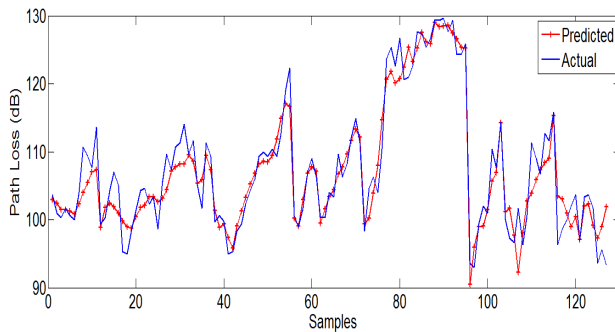


**Figure 9.** Comparison of measured path loss and model predicted path loss (suburban route).

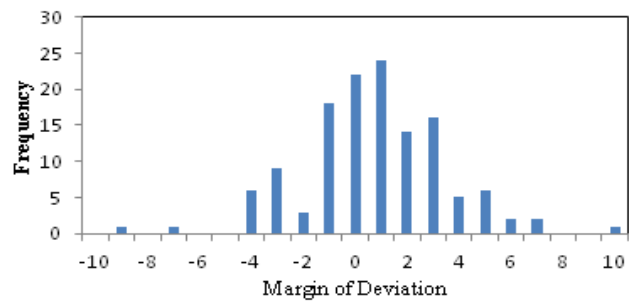


**Figure 10.** Histogram of margin of deviation for ANN path loss model (suburban).

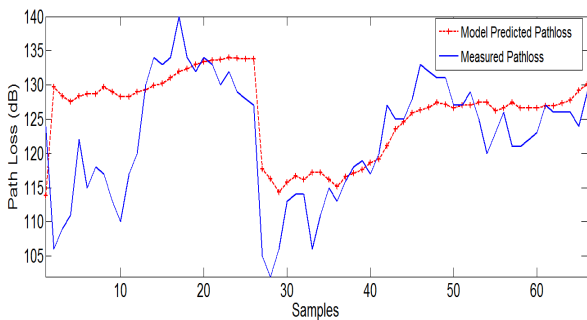


**Figure 11.** Testing of ANN based path loss model using 70 samples (rural route).

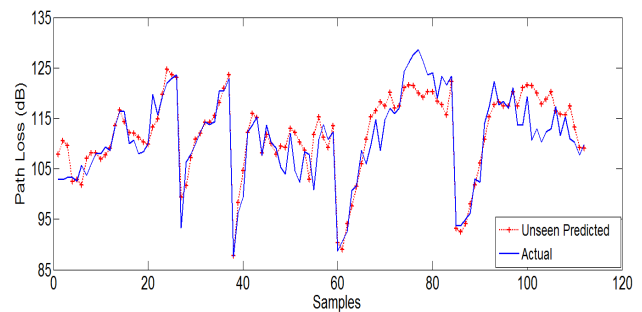


**Figure 12.** Testing of ANN based path loss model using 109 samples (suburban route).

Figure 10 shows high frequency for deviation margin within the range of  $-6$  to  $+6$  which is 96.15% of the total frequency distribution, while 3.85% of the total frequency distribution has margin of deviation within the ranges of  $-7$  to  $-10$  and  $7$  to  $10$ . The margin of deviation and the computed correlation coefficient value of 0.95 show an acceptable accuracy.

Result obtained from testing the ANN based path loss model for rural route using 70 samples of a rural route (Route 2) is shown in Figure 11, while result from the use of the ANN based path loss model for suburban route using 109 samples from suburban routes is shown in Figure 12.

Correlation coefficient values of 0.78 and 0.87 were computed for rural and suburban routes, respectively. The effect of number of training data is observed in Figures 11 and 12. For the ANN based rural route path loss model, Network A, due to the short coverage distance of BTS M01, had 28 training samples (samples 1 to 28 of Figure 7), while Network B had 48 training samples (samples

29 to 76 of Figure 7). The results of testing the ANN based rural route path loss model on Route 2 shown in Figure 11 revealed that 32% of the 25 predicted values for Network A (samples 1 to 25 of Figure 11) had margin of deviation within the ranges of  $-7$  to  $-10$  and  $7$  to  $10$  while 68% had margin of deviation within the ranges of  $-6$  to  $+6$ ; whereas the 48 training samples of Network B gave testing result (samples 26 to 70 of Figure 11) of 8.88% margin of deviation within the ranges of  $-7$  to  $-10$  and  $7$  to  $10$ , and 91.11% margin of deviation within the ranges of  $-6$  to  $+6$ .

#### 4.2. Comparison of Model Predicted Path Loss with Measured Path Loss

The predicted path loss by some basic models and the proposed ANN model were compared with the measured path loss for both the rural and suburban routes. For the rural routes, as shown in Figures 13 and 14, Cost-231 model and Ericsson model greatly overpredict path loss on these routes. Values predicted by Hata and Egli models are observed to be close to the measured path loss values, but the accuracy is low.

For the suburban routes, as shown in Figures 15 to 17, COST-231 and Hata models greatly overpredicted path loss values. Ericsson model is also not in close agreement with the measured path loss values. Path loss predicted values by Egli model are observed to be in close agreement with measured path loss values in Figure 15, but the case is different in Figures 16 and 17.

Figures 18 to 22 reveal that path loss prediction by basic path loss models such as COST-231 model, Ericsson model and Hata model are not in close agreement with measured path loss values. Egli model predicted in close agreement with the measured path loss but only on some routes. Thus, due to disparity in environmental structures, local terrain profiles and weather conditions, path loss

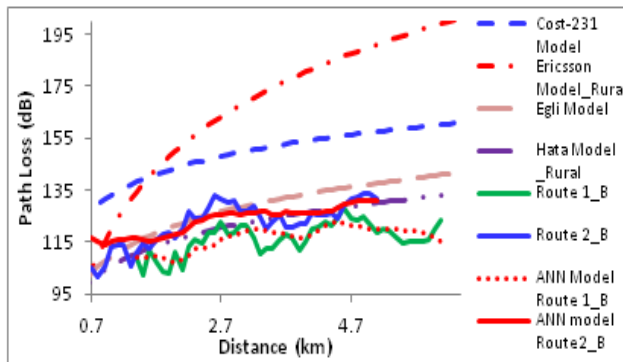


**Figure 13.** Comparison of model predicted path loss and measured path loss on rural routes 1 & 2 (network B).

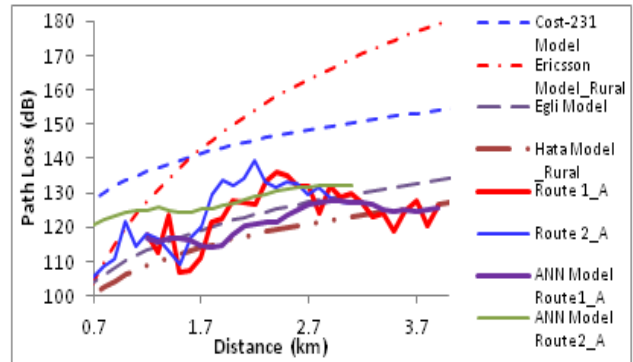


**Figure 14.** Comparison of model predicted path loss and measured path loss on rural routes 1 & 2 (network A).

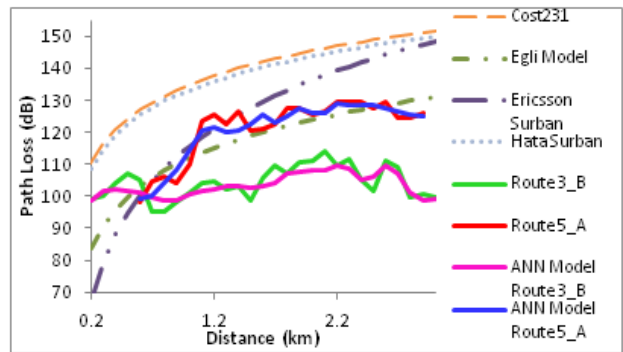


**Figure 15.** Comparison of model predicted path loss and measured path loss on suburban routes 3 & 5 (networks A & B).

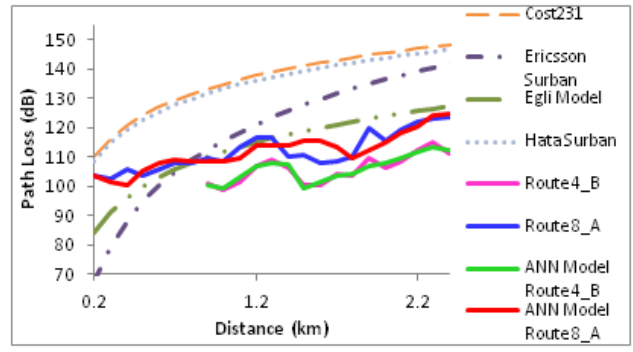


**Figure 16.** Comparison of model predicted path loss and measured path loss on suburban routes 4 & 8 (networks A & B).

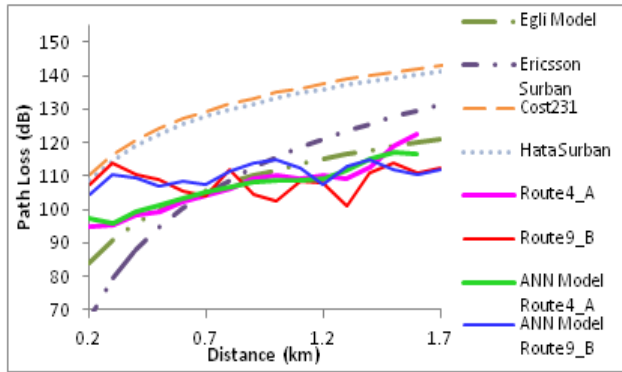


**Figure 17.** Comparison of model predicted path loss and measured path loss on suburban routes 4 & 9 (networks A & B).

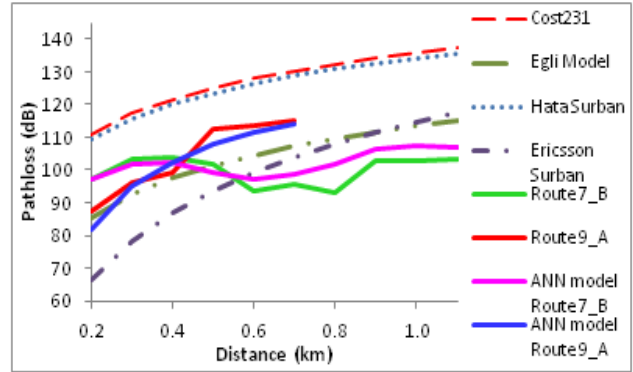


**Figure 18.** Comparison of model predicted path loss and measured path loss on suburban routes 7 & 9 (networks A & B).

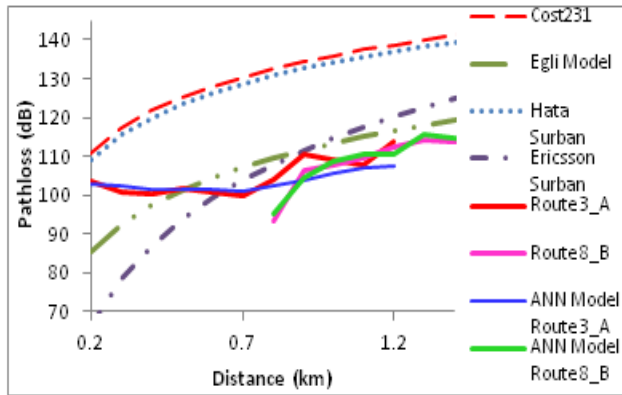


**Figure 19.** Comparison of model predicted path loss and measured path loss on suburban routes 3 & 8 (networks A & B).

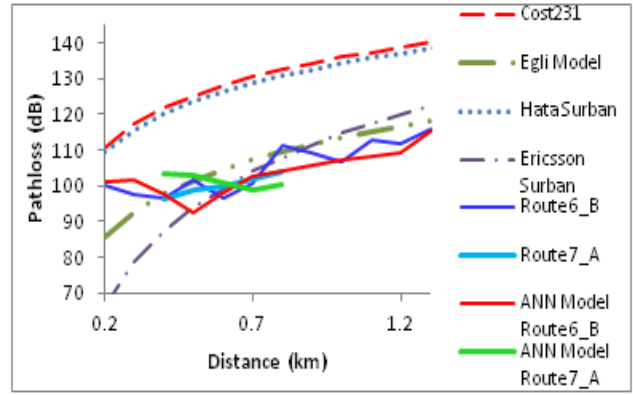


**Figure 20.** Comparison of model predicted path loss and measured path loss on suburban routes 6 & 7 (networks A & B).

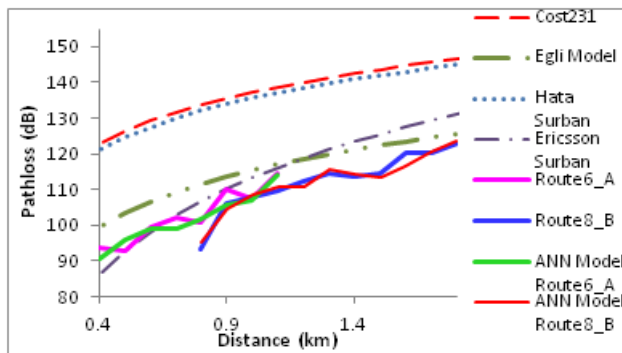


**Figure 21.** Comparison of model predicted path loss and measured path loss on suburban routes 6 & 8 (networks A & B).

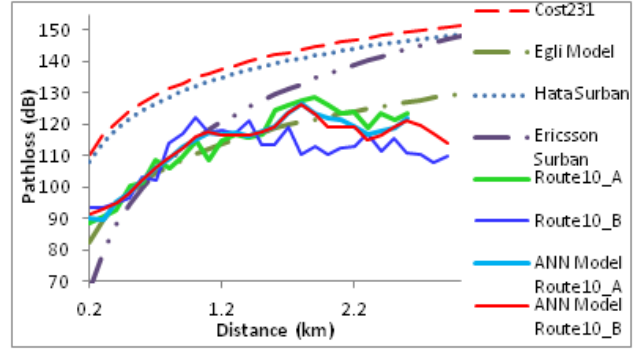


**Figure 22.** Comparison of model predicted path loss and measured path loss on suburban routes 10 (networks A & B).

values predicted for a given environment using existing empirical models such as COST-231 model, Ericsson model, Hata model and Egli model, differ from the optimal model for the given environment. This is in agreement with Ekpenyong et al. [3]; Faruk et al. [4]; Nwalozie et al. [5]; Bakinde et al. [6];

Ogbulezie et al. [12]; Ogbulezie et al. [13]; Chebil et al. [14]. However, the ANN based path loss model predicted in close agreement to measured path loss. Thus, ANN is capable of adequate predictions and this is in agreement with Benmus et al. [16]; Ibeh and Agbo [26]; Litta et al. [27]; Philippopoulos and Deligiorgi [28].

To obtain a quantitative measure of the closeness of the predicted path loss to the measured path loss, [20] proposed the use of Root Mean Square Error (RMSE) given in Equation (14):

$$\text{RMSE} = \sqrt{\frac{\sum_{i=1}^N (t_i - y_i)^2}{N}} \quad (14)$$

where  $N$  is the number of sets in the output data,  $t_i$  the target output, and  $y_i$  the network's output. Hata model showed best performance on the rural routes, with RMSE ranging from 5.05 to 9.30 dB, while Egli model, with RMSE ranging from 3.81 to 8.18 dB, showed best performance on the suburban routes. Detailed results are as shown in Table 2. Model modification by computed MSE technique has been proposed as one of the general solutions to the inaccuracy of basic path loss models in different environments [5, 6, 17]. MSE between measured path loss values and values predicted by Hata model were computed for the rural routes, while the MSE between measured path loss values and Egli model predicted path loss values were computed for the suburban routes using Equation (15):

$$\text{MSE} = (1/N) \left( \sum_{i=1}^N (M_i - P_i)^2 \right) \quad (15)$$

where  $M$  is the measured path loss,  $P$  the predicted path loss, and  $N$  the number of measured data points.

**Table 2.** RMSE for measurement routes.

Area	Route/ Network	COST-231 Model	Hata Model	Egli Model	Ericsson Model	ANN Model
Rural	Route 1 A	23.51	8.30	6.97	36.32	6.53
	Route 1 B	35.63	9.30	15.58	59.66	3.96
	Route 2 A	22.98	8.33	6.06	32.99	7.07
	Route 2 B	25.48	5.05	6.13	42.44	4.63
Suburban	Route 3 A	24.49	22.87	7.33	14.57	3.13
	Route 3 B	36.06	34.44	16.67	27.70	2.89
	Route 4 A	24.29	22.62	4.31	11.24	3.62
	Route 4 B	35.48	33.81	13.57	24.32	1.22
	Route 5 A	21.14	19.50	4.82	11.02	2.64
	Route 6 A	28.18	26.50	5.60	4.39	2.49
	Route 6 B	24.94	23.30	6.04	12.52	4.17
	Route 7 A	23.25	21.64	7.77	18.17	4.25
	Route 7 B	29.05	27.45	10.64	16.18	3.93
	Route 8 A	25.09	23.47	7.73	16.73	3.21
Route 8 B	26.20	24.57	8.18	16.40	4.82	
Route 9 A	26.45	24.90	11.47	18.84	3.48	
Route 9 B	83.36	82.14	69.44	77.57	2.47	
Route 10 A	22.27	20.61	3.81	13.98	2.89	
Route 10 B	26.21	24.59	8.37	19.71	6.16	

Computed MSE value of 70.35 dB, obtained for rural routes, was used to modify Equation (5).

$$\begin{aligned} PL(\text{Rural})_{\text{Hata\_modified}} = & 26.16 \log_{10}(f) - 13.82 \log_{10}(h_b) + \{44.9 - 6.55 \log_{10}(h_b)\} \log_{10}(d) \\ & - 4.78(\log_{10}(f))^2 + 18.33(\log_{10}(f)) + 40.34 \end{aligned} \quad (16)$$

And the computed MSE value of 112.90 dB, obtained for suburban routes, was used to modify Equation (7).

$$PL_{\text{Egli\_Modified}} = 20 \log_{10} f + 40 \log_{10} d - 20 \log_{10} h_b - 36.6 - 10 \log_{10} h_m 20 \quad (17)$$

For the modified Hata model for rural routes, RMSE values ranging from 6.23 to 12.39 dB were obtained, while RMSE values ranging from 3.20 to 50.55 dB were obtained for the modified Egli model for suburban routes. This type of approach of adding computed RMSE/MSE was also compared with the developed ANN based path loss model, and it was also observed that the ANN based path loss model (rural routes) in this work again outperformed the modified Hata model with RMSE ranging from 3.96 to 7.07, while the ANN based path loss model for suburban routes, with RMSE ranging from 1.22 to 6.16 dB, performed better than the modified Egli model.

## 5. CONCLUSION

In this study, using the distance between transmitting antenna and receiving antenna, elevation above sea level of measurement points and transmitting power of reference BTS as input to ANN, ANN based path loss models were developed for rural and suburban routes in Minna and environs.

Comparison of path loss predicted by some basic path loss models and the ANN based path loss model was made. Amongst the basic models, Hata model showed best performance on the rural routes with RMSE ranging from 5.05 to 9.30 dB, but overpredicted path loss on suburban routes, with RMSE ranging from 19.50 to 82.14 dB. Egli model had the best performance on suburban routes, with RMSE ranging from 3.81 to 8.18 dB. COST-231 and Ericsson models overpredicted path loss for both rural and suburban routes. The developed ANN based path loss model performed better than the basic path loss models considered in the study, with RMSE ranging from 3.96 to 7.07 on rural routes and 1.22 to 4.82 on suburban routes. This model is therefore useful for satisfactory prediction of path loss for GSM signals in rural and suburban environments in Minna and environs.

## REFERENCES

1. Reddy, B. M., "Physics of the troposphere," *Handbook on Radio Propagation for Tropical and Subtropical Countries, URSI Committee on Developing Countries, UNESCO Subvention*, 59–77, New Delhi, 1987.
2. Isabona, J., C. C. Konyeha, C. B. Chinule, and G. P. Isaiah, "Radio field strength propagation data and path loss calculation methods in UMTS network," *Advances in Physics Theories and Applications*, Vol. 21, 54–68, 2013.
3. Ekpenyong, M., S. Robinson, and J. Isabona, "Macrocellular propagation prediction for wireless communications in urban environments," *JCS & T*, Vol. 10, No. 3, 130–136, 2010.
4. Faruk, N., A. Ayeni, and Y. A. Adediran, "On the study of empirical pathloss models for accurate prediction of Tv signal for secondary users," *Progress In Electromagnetics Research B*, Vol. 49, 155–176, 2013.
5. Nwalozie, G. C., S. U. Ufoaroh, C. O. Ezeagwu, and A. C. Ejiofor, "Pathloss prediction for GSM mobile networks for urban region of Aba, South-East, Nigeria," *International Journal of Computer Science and Mobile Computing*, Vol. 3, No. 2, 267–281, 2014.
6. Bakinde, N. T., N. Faruk, A. A. Ayeni, M. Y. Muhammad, and M. I. Gumel, "Comparison of propagation models for GSM 1800 and WCDMA systems in selected urban areas of Nigeria," *International Journal of Applied Information Systems (IJAIS)*, Vol. 2, No. 7, 6–13, 2012.
7. Deligiorgi, D., K. Philippopoulos, and G. Kouroupetroglou, "Artificial neural network based methodologies for the spatial and temporal estimation of air temperature," *International Conference on Pattern Recognition Applications and Methods*, 669–578, 2013.
8. Usman, A. U., O. U. Okereke, and E. E. Omizegba, "Instantaneous GSM signal strength variation with weather and environmental factors," *American Journal of Engineering Research (AJSER)*, Vol. 4, No. 3, 104–115, 2015.

9. Sharma, P. K. and R. K. Singh, "Comparative analysis of propagation path loss," *International Journal of Engineering Science and Technology*, Vol. 2, No. 6, 2008–2013, 2010.
10. Ayekomilogbon, O., O. Famoriji, and O. Olasoji, "UHF band radio wave propagation mechanism in forested environments for wireless communication systems," *Journal of Information Engineering and Applications*, Vol. 3, No. 7, 11–16, 2013.
11. Nwawelu, U. N., A. N. Nzeako, and M. A. Ahaneku, "The limitations of campus wireless networks: A case study of University of Nigeria, Nsukka," *International Journal of Networks and Communications*, Vol. 2, No. 5, 112–122, 2012.
12. Ogbulezie, J. C., M. U. Onuu, D. E. Bassey, and S. Etienam-Umoh, "Site specific measurements and propagation models for GSM in three cities in Northern Nigeria," *American Journal of Scientific and Industrial Research*, Vol. 4, No. 2, 238–245, 2013a.
13. Ogbulezie, J. C., M. U. Onuu, J. O. Ushie, and B. E. Usibe, "Propagation models for GSM 900 and 1800 MHz for Port Harcourt and Enugu, Nigeria," *Network and Communication Technologies*, Vol. 2, No. 2, 1–10, 2013b.
14. Chebil, J., A. K. Lwas, M. R. Islam, and A. Zyoud, "Investigation of path loss models for mobile communications in Malaysia," *Australian Journal of Basic and Applied Sciences*, Vol. 5, No. 6, 365–371, 2011.
15. Armoogum, V., R. Munee, and S. Armoogum, "Path loss analysis for 3G mobile networks for urban and rural regions of Mauritius," *Proceedings of the Sixth International Conference on Wireless and Mobile Communications (ICWMC)*, 164–169, 2010.
16. Benmus, T. A., R. Abboud, and M. K. Shater, "Neural network approach to model the propagation path loss for great Tripoli area at 900, 1800 and 2100 MHz bands," *International Journal of Sciences and Techniques of Automatic Control and Engineering*, Vol. 10, No. 2, 2121–2126, 2016.
17. Obot, A., O. Simeon, and J. Afolayan, "Comparative analysis of path loss prediction models for urban macrocellular environments," *Nigerian Journal of Technology*, Vol. 30, No. 3, 50–59, 2011.
18. Seybold, J. S., *Introduction to RF Propagation*, John Wiley & Sons Inc., New York, 2005.
19. Rappaport, T. S., *Wireless Communications: Principles and Practice*, 2nd Edition, Prentice Hall, Upper Saddle River, New Jersey, USA, 2002.
20. Ajose, S. O. and A. I. Imoize, "Propagation measurements and modelling at 1800 MHz in Lagos Nigeria," *International Journal of Wireless and Mobile Computing*, Vol. 6, No. 2, 154–173, 2013.
21. Saunders, S. and A. Aragón-Zavala, *Antennas and Propagation for Wireless Communication Systems*, 2nd Edition, John Wiley & Sons Inc., New York, 2007.
22. Milanovic, J., S. Rimac-Drlje, and I. S. Majerski, "Radiowave propagation mechanisms and empirical models for fixed wireless access systems," *Technical Gazette*, Vol. 17, No. 1, 43–52, 2010.
23. Beale, M. H., M. T. Hagan, and B. O. Howard, *Neural Network Toolbox<sup>TM</sup>*, User Guide, Vol. 7, R2011b, 2011.
24. Aibinu, A. M., A. A. Shafie, and M. J. Salami, "Performance analysis of ANN based YCbCr skin detection algorithm," *Procedia Engineering*, Vol. 41, 1183–1189, 2012.
25. Eichie, J. O., O. D. Oyedum, M. O. Ajewole, and A. M. Aibinu, "Artificial neural network model for the determination of GSM rxlevel from atmospheric parameters," *Engineering Science and Technology*, retrieved from <http://dx.doi.org/10.1016/j.jestch.2016.11.002>, 2016.
26. Ibeh, G. F. and G. A. Agbo, "Estimation of tropospheric refractivity with artificial neural network at Minna, Nigeria," *Global Journal of Science Frontier Research Interdisciplinary*, Vol. 2, No. 1, 8–14, 2012.
27. Litta, A. J., S. M. Idicula, and U. C. Mohanty, "Artificial neural network model in prediction of meteorological parameters during premonsoon thunderstorms," *International Journal of Atmospheric Sciences*, Vol. 10, 1–14, 2013.
28. Philippopoulos, K. and D. Deligiorgi, "Application of artificial neural networks for the spatial estimation of wind speed in a coastal region with complex topography," *Renewable Energy*, Vol. 39, 75–82, 2012.